

Voice Instabilities due to Source-Tract Interactions

Haralambos Hatzikirou¹, W. Tecumseh Fitch², Hanspeter Herzel¹

- 1) Institute for Theoretical Biology, Humboldt Universität zu Berlin, Invalidenstrasse 43, D-10115 Berlin, Germany
- 2) School of Psychology, St. Andrews University, St. Mary's College, Fife, KY16 9JP, Scotland

Abstract

Interactions of voice source and vocal tract resonances are of particular interest with respect to register transitions and bioacoustics. There is experimental evidence that singing into a tube generates nonlinear phenomena around matching frequencies of the pitch and the first formant. In the present study, we analyze a simplified two-mass model coupled to a straight tube. The essential parameters of the systems are varied systematically to localize instability regions in parameter space. The resulting bifurcation diagrams reveal subharmonic vibrations and deterministic chaos if the pitch and the first formant coincide. The computer simulations closely resemble published experimental observations. Furthermore, we demonstrate the role of coupling strength as the cause of instability. Small tube cross sectional areas and overcritical pressures are responsible for additional instability regions around second pitch harmonic and formant resonance. The results indicate that under certain circumstances source-tract interactions induce quite complex voice instabilities, even for symmetric vocal folds. These include frequency jumps, subharmonic regimes and chaos. The possible relevance for the soprano whistle voice and animal vocalization is discussed.

1. Introduction

There has been a long debate on the role of source-tract coupling in human voice production [1, 2]. In many musical instruments the eigenfrequencies of the resonators dictate the pitch, implying a rather strong coupling. Early experiments with excised larynges indicate, however, that vocal fold vibrations are fairly autonomous [3, 4]. Diverse register transitions and voice instabilities have been found in isolated larynges [5]. Consequently, two-mass models of vocal folds [6] show robust oscillations without sub- and supraglottal resonators [7]. Recently, register-like phenomena have been described in a two-mass model without vocal tract [8]. Moreover, at high driving pressures the simplified two-mass model displays transitions to chaotic dynamics [9]. All these observations stress the relative independence of the voice source and the vocal tract. Consequently, the source-tract theory gives a good approximation to human speech [10]. The coupling is quite weak due to the following reasons:

- The phase shift of upper and lower edge of the vocal folds allows transfer of energy from the air flow to the vibrating folds, modeled by the two-mass approximation [11, 12]. Hence support by resonators is not necessary for self-oscillation.

- The sudden increase of the area immediately above the glottis (the "epilarynx") leads to a large impedance change and a reduced feedback from vocal tract resonators.
- At least for chest voice there is a clear separation of pitch frequencies (100-250 Hz) and first formant (300-1000 Hz) [13].

These considerations immediately suggest mechanisms that could enhance source-tract interactions: a narrow epilaryngeal tube increases the feedback, and comparable frequencies of source and tract may lead to resonance phenomena. Both situations can be quite relevant. Relatively narrow epilaryngeal tubes have been measured using MRI [14, 15] and for the so-called "whistle voice" a narrow epilarynx seems to be essential [5, 16, 17]. For high singing voices the pitch and formant frequencies are no longer separated. There are indications that vocal improvisors exploit source-tract interactions to produce diverse nonlinear phenomena [18]. The discussion of source-tract coupling is also of crucial importance in animal vocalizations. Due to an elongated vocal tract [19] or high pitches, overlap between source and vocal tract frequencies may occur and morphological peculiarities might further strengthen source-tract interactions. For example, vocal membranes enlarge the effective area of vocal folds and allow a strong feedback of vocal tract pressures [20]. In this paper we reconsider a classic study of source-tract interactions [21, 22]. Kagen and Trendelenburg [22] experimentally studied artificial prolongations of the vocal tract using glass and metal tubes of 50 cm, 75 cm and 100 cm length. They found on the one hand constructive resonances with large amplitudes and pronounced harmonics. On the other hand, they observed that "disturbances of sound appear when the sung pitch corresponds to that of the fundamental tone or an overtone of the tube system" [22]. They describe "jumps in pitch" and "tremolo-like alterations in amplitude and slight changes in rhythmic frequency". From the point of view of nonlinear dynamics these observations are not surprising. The theory of nonlinear coupled oscillators predicts that different entrainment regimes, frequency jumps, subharmonic bifurcations, toroidal oscillations and deterministic chaos can be expected. In the following we introduce a simple biomechanical model of "singing into a tube" and study the bifurcations and attractors in that system. Bifurcation diagrams display the role of parameters such as subglottal pressure, pitch, tube diameter and tube length.

2. Modeling Source-Tract Interactions

There are very detailed models of vocal fold vibrations [23, 24] and of sub- and supraglottal resonators [15, 25]. These complex models contain many dynamic variables and parameters. In order to study the very basic mechanisms of voice instabilities we choose a highly reduced model version - a combination of the simplified two-mass model [7, 9, 26, 27] with a straight tube. Such a "caricature" of the voice producing system allows us the focus on the essential features of the dynamics. Varying pitch and tube length leads to quite complex bifurcation scenarios that resemble experimental studies of "singing into a tube". The derivation of the relevant biomechanical and aerodynamical equations is discussed in detail elsewhere [6, 7]. Here we present the system of equations and primarily discuss the interactions between the simplified two-mass model and the tube. The default parameters are given in the Appendix. Two second order equations model the coupled vibrations x_1 and x_2 , that represent the amplitude of lower and upper mass in the vibratory (horizontal) plane.

$$m_1 \frac{d^2 x_1}{dt^2} + r_1 \frac{dx_1}{dt} + \Theta(-a_1) c_1 a_1 2l + k_1 x_1 + k_c (x_1 - x_2) = P_1 l g d_1, \quad (1)$$

$$m_2 \frac{d^2 x_2}{dt^2} + r_2 \frac{dx_2}{dt} + \Theta(-a_2) c_2 a_2 2l + k_2 x_2 + k_c (x_2 - x_1) = P_2 l g d_2, \quad (2)$$

The instantaneous glottal area of each mass is described by $a_i = a_{0i} + 2l_g x_i$; $i = 1, 2$: As in [7] we neglect biomechanical nonlinearities but include additional restoring forces in case of collision, i.e. for $a_i < 0$. These terms are "turned on" using the Heaviside function:

$$\Theta(x) = \begin{cases} 1, & x > 0 \\ 0, & x \leq 0 \end{cases}$$

The coupling to the resonating tube is given via the aerodynamic pressures P_1 and P_2 acting on the vocal folds. In case of a totally closed glottis ($a_1, a_2 < 0$) both pressures are set to zero. If only the upper part is closed ("converging glottis") ($a_2 < 0$), P_1 equals the subglottal pressure P_S : For a closed lower part ("diverging glottis") ($a_1 < 0$) the pressure P_2 is given by the vocal tract input pressure $P_T = (u_g - u_1)/C$. Now we discuss the case of non vanishing glottal airflow U_g . Then the pressure P_1 is derived from the Bernoulli equation:

$$P_1 = P_S - \frac{\rho}{2} \left(\frac{U}{a_1} \right)^2, \quad (3)$$

As discussed in earlier work [7], we assume that an air jet is formed at the point of minimum area leading to an abrupt pressure decay. For a divergent glottis ($a_2 > a_1 > 0$) we get $P_2 = P_1 = P_T$ and for a convergent glottis:

$$P_2 = P_S - \frac{\rho}{2} \left(\frac{U}{a_2} \right)^2$$

The pressure P_2 serves as input for the equations governing the flow and pressure in the tube and at the mouth. Along the

lines of Flanagan [28], we use the following equations to describe the glottal flow U_g , the flow in the tube U_1 and at the mouth U_m :

$$\frac{du_g}{dt} = \Theta(a_{\min}) U_g, \quad (4)$$

$$L \frac{dU_g}{dt} + R U_g + \frac{1}{C} (u_g - u_1) = P_2, \quad (5)$$

$$\frac{du_1}{dt} = U_1, \quad (6)$$

$$L \frac{dU_1}{dt} + L_m \left(\frac{dU_1}{dt} - \frac{dU_m}{dt} \right) + R U_1 + \frac{1}{C} (u_1 - u_g) = 0, \quad (7)$$

$$\frac{du_m}{dt} = U_m, \quad (8)$$

$$L_m \left(\frac{dU_m}{dt} - \frac{dU_1}{dt} \right) + R_m U_m = 0, \quad (9)$$

The auxiliary variables u_g , u_1 and u_m simplify the equations. The tube parameters L , R and C depend on tube area A and length l (see Appendix).

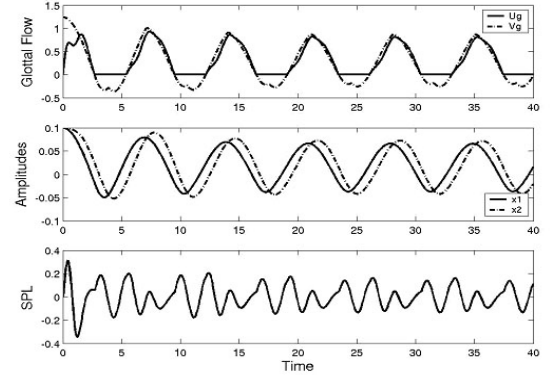


Figure 1: *Simulated model variables at default parameters. The first graph represents the glottal volume flow U_g and the $V_g = (2P_S/\rho)^{1/2} a_{\min}$. The graph below shows the oscillations of the source two masses x_1 and x_2 . Finally, we plot the time derivative of the mouth airflow as an approximation of the sound pressure level (SPL).*

Figure 1 shows simulations of the model using default parameters. In the upper graph we present also the approximation $V_g = (2P_S/\rho)^{1/2} a_{\min}$. The positive values of this term would represent the glottal flow in the simplified two-mass model without vocal tract. It can be seen that U_g and V_g are quite similar pointing to the finding that under normal conditions there is only a minor feedback of the vocal tract. Since $L \sim 1/A$, $1/C \sim 1/A$ and $R \sim 1/A^2$ (see Appendix) we see from Eq.5 that a large tube area leads to vanishing interactions. On the contrary, small epilaryngeal areas enhance the feedback and increase the likelihood of the voice instabilities, as discussed below.

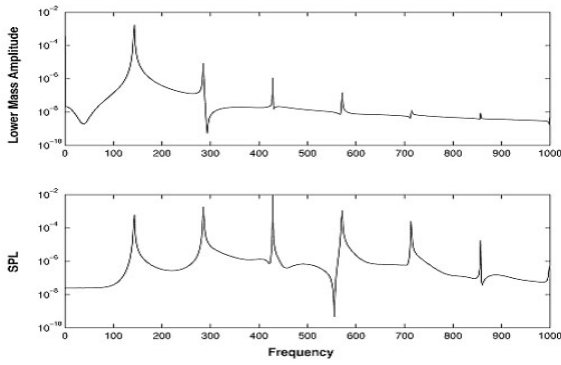


Figure 2: Power spectra of lower mass amplitude and SPL, using default parameters as in Fig.1.

In Figure 2 we visualize the spectra of the vocal fold vibrations (upper graph) and the corresponding acoustic output at the mouth dU_m/dt (lower graph). Since the default length of the tube is 17.5 cm harmonics around the x_1 formant frequency at 500 Hz are relatively strong. Since the formant frequency is inversely proportional to the tube length, a much longer tube leads to a formant frequency in the range of the pitch (about 100 Hz). In the following section, we discuss voice instabilities induced by the resonant interactions of pitch and formant of a prolonged tube.

3. Bifurcations and Attractors

In order to detect voice instabilities due to varying system parameters, we plot the maxima of x_1 -oscillations versus the parameter of interest. An increase of subglottal pressure leads to an onset of oscillation at about $PS = 0.003$ via a Hopf bifurcation, but no other bifurcations are observed [29]. Increasing the tube length l leads to sudden transitions of the dynamical behavior. These bifurcations are displayed in Figure 3.

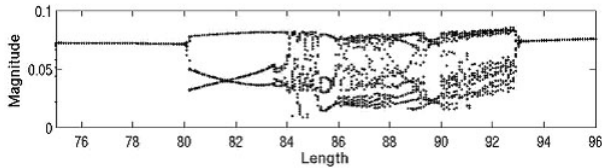


Figure 3: Bifurcation diagram of lower mass amplitude x_1 against the tube length l . The control parameter is varied from 75 to 96 cm.

The parameter range with instabilities is between $l=80$ cm and $l=93$ cm corresponding approximately to a 1:1 resonance of pitch and first formant. Despite the simplicity of the model we find a quite complex bifurcation diagram. At about $l=80$ cm a sudden transition to a sub harmonic regime is observed. This transition is associated with period-doubling in the time domain (compare Fig. 4) or an octave jump in the frequency domain (see Fig. 5). Around $l=84$ cm the amplitudes of x_1 start to fluctuate irregularly in a wide range. In between small

windows of complex periodic vibrations are visible. These alternations of "deterministic chaos" and "periodic windows" are well-known from nonlinear dynamical systems such as the logistic map [30] or coupled nonlinear oscillators [31, 32].

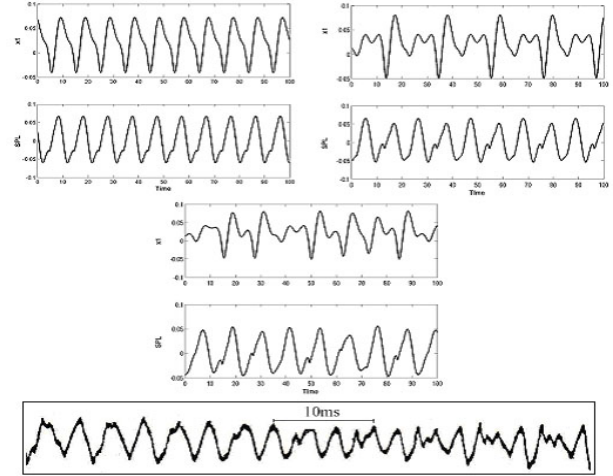


Figure 4: The graph shows time series pairs of lower mass amplitude and SPL at $l = 76, 81.5, 90$ cm. The lower graph represents the redrawn experimental recording of singing into a tube of 100 cm length [22].

Figure 4 shows representative time series of periodic, subharmonic and chaotic oscillations. The last graph in Figure 4 is an experimental recording made by singing into a 100 cm long tube (redrawn from Ref. [22]). Those authors reported diverse voice instabilities in an interval of 1-2 halftones around the pitch formant resonance. The instability range in our simulations is quite similar.

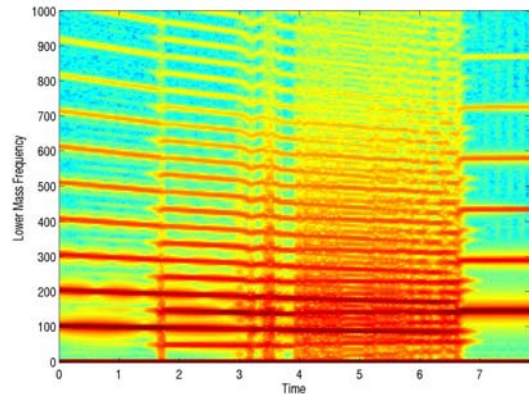


Figure 5: The spectrogram corresponds to the bifurcation diagram of Fig.3. It shows the frequency changes of x_1 due to the linear increase of length, l [75; 96].

Now we analyze some representative simulations in some detail using tools of nonlinear dynamics. Figure 6 shows phase portraits of periodic, subharmonic and chaotic attractors. A recurrence plot of subsequent maxima of x_1 is topologically equivalent to a Poincare section through the attractor. The

corresponding plot in Figure 7 reveals the complex pattern associated with the chaotic attractor. The amplitude spectra for these selected parameter values are presented in Figure 8. Subharmonics and broad-band components are clearly visible. These representations of periodic, subharmonics and chaotic regimes illustrate that the vocal instabilities due to source-tract interactions are indeed characteristic features of a chaotic dynamical system.

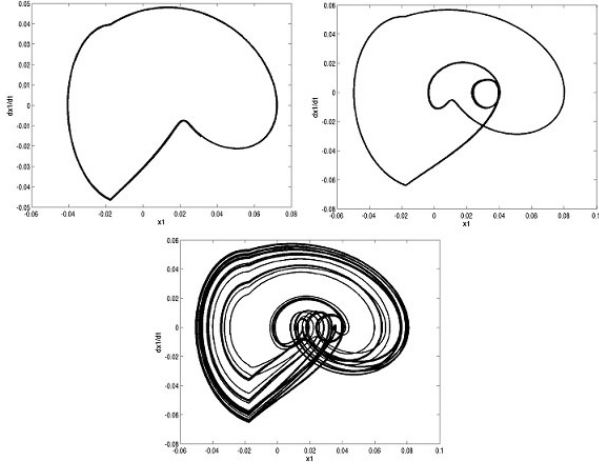


Figure 6: The graph presents the attractors of the simulations shown in Fig. 5 in the plane of $(x_1; dx_1/dt)$. The upper left diagram shows the limit cycle of periodic vocal folds vibrations. The folded attractor indicates a subharmonic regime at $l=81.5$ cm. The lower diagram corresponds to chaotic oscillations at $l=90$ cm.

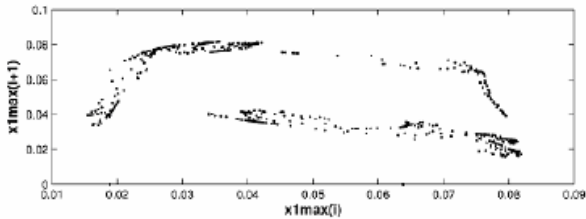


Figure 7: The plot visualizes a return map, i.e. consecutive maxima of x_1 are plotted at the length of $l=90$ cm. The plot makes evident that we deal with a chaotic attractor.

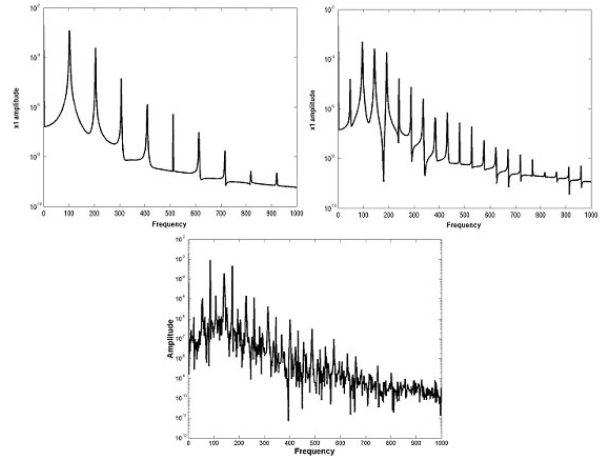


Figure 8: The graph shows Fourier spectra of x_1 from the simulation of Fig.4. The upper left plot depicts a regular spectrum of $l=76$ cm. The second graph contains subharmonics due to period-doubling. The last graph shows an unstructured spectrum of the chaotic regime.

In the following we discuss the necessary requirements to get voice instabilities due to source-tract interactions. As outlined in the introduction, a sufficiently strong interaction is necessary. Thus we can predict that instabilities is appear for small subglottal pressures and for large tube areas. In both cases the interactions are weakened. Figure 9 shows that instabilities indeed require overcritical subglottal pressures and a relatively small tube area. Recent measurements indicate that the epilaryngeal tube can have an area as low as 1 cm^2 [15]. Such a narrow tube can enhance voice instabilities [2]. A spectral bifurcation diagram for varying tube length with an area of only 1 cm^2 displays enlarged instability regions (see Fig. 10). Interestingly, there are also instabilities around $l=35$ cm related to a resonance of the second source harmonic with the lowest formant.

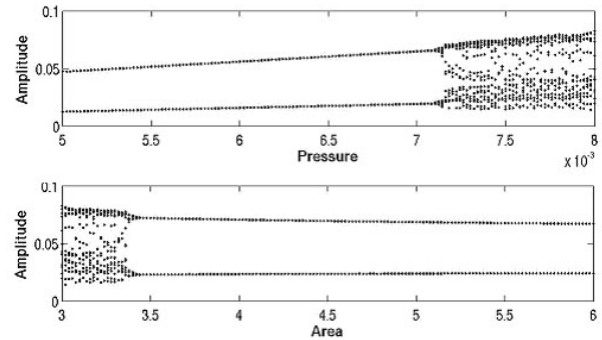


Figure 9: The graph presents two bifurcation diagrams of x_1 that exemplify the role of coupling for the instability generation at the tube length of 90 cm. The upper graph shows that the decrease of pressure leads to regular oscillations. The lower one reveals that a small increase of the tube cross sectional area is sufficient to eliminate the complex patterns of x_1 vibrations.

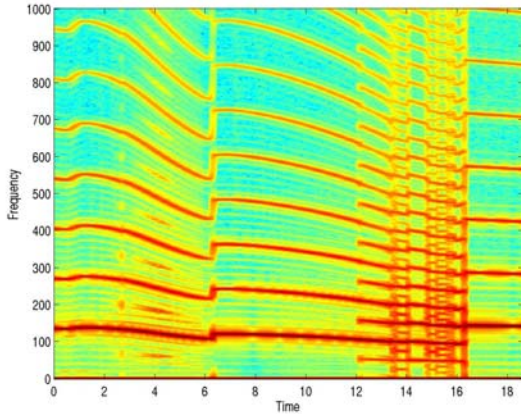


Figure 10: Bifurcations at strong coupling (tube area $A = 1 \text{ cm}^2$). The graph shows a spectrogram of x_1 during a tube length variation from 20 to 85 cm, started from default initial conditions. The interactions of the formant with the second harmonic lead to a subharmonic regime around $l=35 \text{ cm}$.

The simulated instabilities strongly resemble early experiments by Kagen and Trendelenburg [22]. It is surprisingly easy to reproduce their findings. The spectrogram in Figure 11 shows our own experiment involving singing into a tube. The metal tube has a length of 160 cm and an inner diameter of about 2.5 cm. Gradually increasing the pitch with a sufficiently loud voice leads reproducibly to voice instabilities. In order to obtain the corresponding simulation we varied the pitch using a tuning parameter Q (see [20]) at a given tube length of $l=90 \text{ cm}$. The resulting spectrogram is displayed in Figure 12. We observed frequency pulling of the source frequency by the resonator and subsequent sudden jumps to subharmonic regimes. Thus our simplified model is able to reproduce essential features of voice instabilities due to source-tract interactions found experimentally.

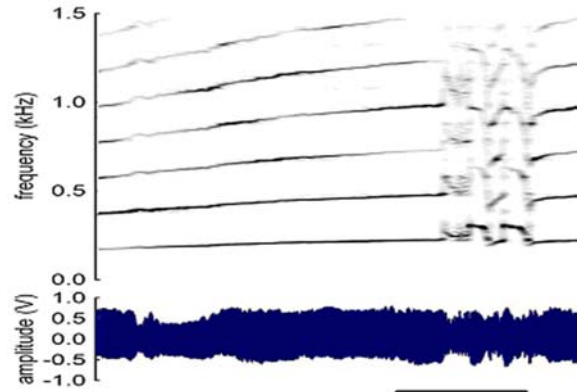


Figure 11: Experimental spectrogram obtained by "singing into a tube" of length 160 cm and inner diameter 2.5cm.

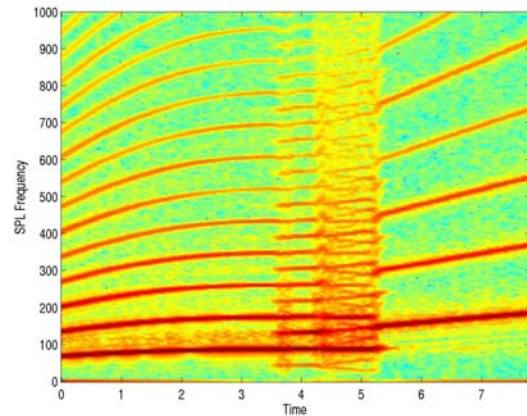


Figure 12: The spectrogram presents the variations of SPL frequency with respect to the change of pitch parameter Q 2 [0:5; 1:3], at a length of 90 cm. It resembles the experiments of singing into a tube. One can observe subharmonics and frequency jumps while the pitch is increased.

4. Summary

In this study we investigated the circumstances under which source-tract interactions lead to voice instabilities. Such interactions might be particularly relevant for the singing voice [18] and certain animal vocalizations [33]. Since a comprehensive bifurcation analysis is a complex endeavor even in such simple systems as the logistic map [30] or a periodically driven oscillator [34] we studied a rather simple model - the two-mass model [7] coupled to a straight tube. The parameter values of this system were varied systematically to localize regions of voice instabilities. An increase of subglottal pressure at the default configuration leads to an oscillation onset (Hopf bifurcation) around $P_S = 3 \text{ cmH}_2\text{O}$, but no further bifurcations were found. Variations of the tube length or the pitch frequency revealed instability regions close to frequency

matches between source and tube. In many cases coexisting attractors were observed, implying sudden jumps of the dynamics as parameters are varied [29]. The instabilities around resonances extend typically over a range of 1-2 halftones. The results of our simulation closely resemble earlier experimental observations [22] and our own experiments (see Fig. 11). In both the simulations and the experiments, subharmonics, frequency jumps and more complex vibration patterns (chaos or modulations) have been observed.

In a computer model parameters can be varied easily in order to study the underlying mechanisms of the instabilities. A strong coupling between source and tract is always necessary. For a very narrow tube we even found bifurcations at the resonance between the second harmonic of the source and the lowest formant frequency of the tube. The coupling of source and tract has to be strong enough to generate bifurcations. Instabilities occur for a relatively narrow tube since a small area leads to a reduced impedance change at the glottal outlet and thus stronger coupling. Moreover, overcritical subglottal pressures are required to get instabilities since large amplitudes imply that nonlinearities become relevant and lead to a stronger feedback of the vocal tract. Since voice instabilities occur only under specific circumstances the source-filter theory of Fant [10] remains a reasonable approximation for the normal speaking (or "chest") voice. At high pitches and for a loud pressed voice, interactions of source and tract are enhanced. Source-tract interactions are presumably relevant to explain transitions from a falsetto voice to the "whistle registers" of soprano singers [16, 17]. Moreover, experimental vocal improvisers may exploit source-tract coupling to produce nonlinear phenomena [18].

Interactions of source and vocal tract may be particularly relevant in bioacoustics. Animal vocalizations exhibit a wide range of pitches and diverse vocal tract geometries [35, 36, 37, 38]. Furthermore, nonlinear phenomena are widespread in animal voices [19, 39]. In particular, air sacs might act as a resonator to diversify the vocal repertoire of some species. In birds the voice producing organ - the syrinx - is located below the trachea providing an additional resonator. The syrinx has been modeled by a two-mass model as well [40, 41]. Finally, some species greatly elongate the vocal tract during loud vocalizations, thus lowering formant frequencies [19]. Often, nonlinearities can be observed during such calls. Consequently, our model appears relevant to understanding the physics underlying certain bird and mammal vocalizations, which may differ from the normal human voice.

In general, nonlinear phenomena are an essential part of vocal production. There are many possible mechanisms to induce voice instabilities such as left-right asymmetries [7, 27], desynchronization of vibratory modes [42], or additional vibrating structures (vocal membranes, ventricular folds). In this paper we have demonstrated that a destructive interference between vocal fold oscillations and tract resonances can lead to nonlinear phenomena as well. Future experimental and theoretical studies are necessary to provide a comprehensive picture of the variety of voice instabilities.

5. References

- [1] Titze, I.R.: Principles of Voice Production, Prentice-Hall, 1994.
- [2] Laje, R., Gardner, T.J., Mindlin, G.B.: Continuous model for vocal fold oscillations to study the effect of the feedback. *Physical Review E*, 64:056201, 2001.
- [3] Trendelenburg, W., Wullstein, H.: Untersuchungen ueber die Stimmbandschwingungen. *Sitzungsgeber. d. Preuss. Ak. d. Wiss.*, XXI, 399-426, 1935.
- [4] Van den Berg, J.: Myoelastic-aerodynamic theory of voice production. *J. Acoust. Soc. Am.*, 1:227-244, 1957.
- [5] Berry, D.A., Herzel, H., Titze, I.R., Story, B.: Bifurcations in excised larynx experiments. *J. of Voice*, 10:129-138, 1996.
- [6] Ishizaka, K., Flanagan, J.L.: Synthesis of voiced sounds from a two-mass model of vocal cords, *Bell Syst. Tech.*, 51:1233-1268, 1972.
- [7] Steinecke, I., Herzel, H.: Bifurcation in an asymmetric vocal fold model. *J. Acoust. Soc. Am.*, 97:1571-1578, 1995.
- [8] Sciamarella, D., d'Alessandro, C.: An acoustic analysis of a symmetrical two-mass model. *Acta Acoustica*, 2004.
- [9] Jiang, J., Zhang, Y.: Modeling of chaotic vibrations in symmetrical vocal folds. *J. Acoust. Soc. Am.*, 110:2120-2128, 2001.
- [10] Fant, G.: *Acoustic theory of speech*. Mouton, Paris, 1960.
- [11] Stevens, K.N.: Physics of laryngeal behavior and larynx modes. *Phonetica*, 34:246-276, 1977.
- [12] Titze, I.R.: The physics of small-amplitude oscillation of the vocal folds, *J. Acoust. Soc. Am.*, 83:1536-1552, 1988.
- [13] O. Shaughnessy, P.: *Speech communications, human and machine*. pp 67-71, Addison-Wesley, NY, 1987.
- [14] Story, B.H., Titze, I.R., Hoffman, E.A.: Vocal tract area functions from MRI, *J. Acoust. Soc. Am.*, 100:537-554, 1996.
- [15] Apostol, L., Perrier, P., Bailly, G.: A model of acoustic interspeaker variability based on the concept of formant-cavity affiliation. *J. Acoust. Soc. Am.*, 115:337-351, 2004.
- [16] Walker, J.S.: An investigation of the whistle register in female voice. *J. of Voice*, 2:140-150, 1988.
- [17] Miller, D.G., Schutte, H.K.: Physical definition of the "Flageolet Register". *J. of Voice*, 7:206-212, 1993.
- [18] Neubauer, J., Edgerton, M., Herzel, H.: Nonlinear phenomena in contemporary vocal music. *J. of Voice*, 18:1-12, 2004.
- [19] Fitch, T.W., Reby, D.: The descended larynx is not uniquely human. *Proc. R. Soc. Lond. B.*, 268:1669-1675, 2001.
- [20] Mergell, P., Fitch, T.W., Herzel, H.: Modeling the role of non-human vocal membranes in phonation. *J. Acoust. Soc. Am.*, 105:2020-2028, 1998.
- [21] Weiss, D.: Ein Resonanzphaenomen der Singstimme. *Monatsschr. f. Ohren heilk. u. Lar.-Rhinol.*, 66:964-967, 1932.
- [22] Kagen, B., Trendelenburg, W.: Zur Kenntnis der Wirkung von kuenstlichen Ansatzroehren auf die Stimmschwingungen. *Archiv fuer die Gesamte Phonetik*, 3:124-150, 1937.
- [23] Alipour-Haghighi, F., Titze, I.R.: Elastic models of vocal fold tissues. *J. Acoust. Soc. Am.*, 90:1326-1331, 1991.

- [24] Pelorson, X., Hirschberg, A., van Hassel, R. R., Wijnands, A.P.J., Auregan, Y.: Theoretical and experimental study of quasi-steady flow separation within the glottis during phonation. Application to a modified two-mass model. *J. Acoust. Soc. Am.*, 96:3416-3431, 1994.
- [25] Story, B.H., Titze, I.R., and Hoopman, E.A.: The relationship of vocal tract shape to three voice qualities. *J. Acoust. Soc. Am.*, 109, 1651-1667, 2001.
- [26] Mergell, P., Herzel, H.: Modeling biphonation—the role of the vocal tract. *Speech Communication*, 22:141-154, 1997.
- [27] Tigges, M., Mergell, P., Herzel, H., Wittenberg, T., Eysholdt, U.: Observation and modeling glottal biphonation. *Acta Acustica* 83:707-714, 1997.
- [28] Flanagan, J.L.: *Speech analysis, synthesis and perception* Springer Berlin, Heidelberg, NY, 1972.
- [29] Hatzikirou, H.: Bifurcation analysis of a vocal fold model coupled to resonators. Master Th., TU Kaiserslautern, ITB, Berlin 2004.
- [30] May, R.M., Oster, G.F.: Bifurcations and dynamic complexity in simple ecological models. *Amer. Nature*, 110: 573-599, 1976.
- [31] Berge, P., Pomeau, Y., Vidal, C.: *Order within chaos: Towards a deterministic approach to turbulence*. Herman, Paris, 1984.
- [32] Glass, L., Mackey, M.: *From clocks to chaos: The rhythms of life*, Princeton University Press, 1988.
- [33] Fitch, W.T., Neubauer, J., Herzel, H.: Calls out of chaos: the adaptive significance of nonlinear phenomena in mammalian vocal production. *Animal Behaviour*, 63:407-418, 2002.
- [34] Parlitz, U., Lauterborn, W.: Superstructure in the bifurcation of Duffing equation: $d^2x/dt^2 + Ddx/dt + x + x^3 = f \cos(\omega t)$. *Physics Letters A*, 107A(8):351-355, 1985.
- [35] Negus, V.E.: *The comparative anatomy and physiology of the larynx* Hafner Publishing Company, NY, 1949.
- [36] Harrison, D.F.N.: *The anatomy and physiology of the mammalian larynx*. Cambridge University Press, NY, 1965.
- [37] Bradbury, J., Lehrencam, S.: *Principles of animal communication*. Sinauer Assoc. Inc., 1998.
- [38] Fitch, W. T., Hauser, M. D.: Unpacking "Honesty": Vertebrate vocal production and the evolution of acoustic signals. in *acoustic communication* (Ed. by Simmons, A. M., Fay, R. F. & Popper, A. N.), pp.65-137. New York: Springer, 2002.
- [39] Wilden, I., Herzel, H., Peters, G., Tembrock, G.: Subharmonics, biphonation and deterministic chaos in mammal vocalization. *Biocoustics*, 9:171-196, 1997.
- [40] Fee, M.S., Shairman, B., Pesaran, B., Mitra, P.P.: The role of nonlinear dynamics of the syrinx in the vocalization of a songbird. *J. Acoust. Soc. Am.*, 95:67-71, 1998.
- [41] Laje, R., Gardner, T.J., Mindlin, G.B.: Neuromuscular control of vocalization in birdsong: A model. *Physical Review E*, 65:051921, 2002.
- [42] Berry, D.A., Herzel, H., Titze, I.R., Krischer, K.: Interpretation of biomechanical simulations of normal and chaotic vocal fold oscillations with empirical eigenfunctions. *J. Acoust. Soc. Am.*, 95:3595-3604, 1994.

6. Appendix

6.1. Model Parameters

All the values are given in cm, g, ms and their corresponding combinations. The model is comprised of the two-mass model [7] coupled to a straight tube, represented by a transmission line [28]. The parameters concerning the vocal fold model are identical to the simplified two-mass model of Steinecke & Herzel [7]. The tube parameters are obtained from the work of Isizaka-Flanagan [6]. The following phonation conditions are referred to as "default parameters".

Subglottal pressure: $P_s = 0:008$
 Masses: $m_1 = 0:125$; $m_2 = 0:025$
 Damping constants: $r_1 = r_2 = 0:02$
 Spring constants: $k_1 = 0:08$; $k^2 = 0:008$
 Coupling constant: $kc = 0:025$
 Collision constants: $c^1 = 3k_1$; $c_2 = 3k_2$
 Mass thickness: $d1 = 0:25$; $d2 = 0:05$
 Glottis length: $l_g = 1:4$
 Air density: $\rho = 0:00113$
 Air speed: $c = 35$
 Rest glottal areas: $a_{01} = 0:05$; $a_{02} = 0:05$
 Tube length: $l = 17,5$
 Tube cross sectional area: $A = 3$
 Tube inductance: $L = l \rho / 2A$
 Tube capacitance: $C = lA / \rho c^2$
 Tube resistance: $R = ATT S(\rho \mu \omega)^{1/2} / A^2$
 Resistance correction coefficient: $ATT = 25$
 Air viscosity: $\mu = 1,8 \cdot 10^6$
 Radian frequency of m_1 : $\omega = (k_1 / m_1)^{1/2}$
 Mouth inductance: $L_m = 8 \rho (\pi A)^{1/2} / 3\pi$
 Mouth resistance: $R_m = 128 \rho c / 9 \pi^2 A$

6.2. Simulation Details

The initial values for all of the simulations were: $x_{01} = x_{02} = 0,1$ and vanishing velocities and flows. To obtain bifurcation diagrams, we integrate the system 500 ms to reduce the transients. During the next 100 ms maxima are calculated using spline interpolation and plotted (see e.g. Fig 3). For the next parameter values we use the final state of the preceding simulations as initial conditions and integrate another 100 ms. The parameters of our spectrogram calculations are as follows:

Sampling rate: 20 kHz
 Window length: 4092 sample points
 Overlap: 4000 sample points
 Windowing: Hanning